Supporting Information

Sustainable and Lignin-Assisted Polyester with Exceptional Optical Filtering via Highly Atom-Efficient In-Situ Polymerization Strategy

Shi Liu[a], Conghui Mi[a], Yuxuan Qiu[a], Zhihan Tong[a], Jiajun Liu[a], Jinsong Sun[a], Xiaoxue Song[b], Qinqin Xia[a]*and Haipeng Yu[a]**

[a]Laboratory of Bio-based Material Science and Technology of Ministry of Education, Northeast Forestry University, Hexing Road 26, Harbin, 150040, P.R. China

[b]College of Home and Art Design, Northeast Forestry University, Harbin, 150040, PR China

*Corresponding authors: yuhaipeng20000@nefu.edu.cn, 2018xiaqinqin@nefu.edu.cn, songxiaoxue@nefu.edu.cn

Transparent PDES was synthesized by heating citric acid and 1.6-hexanediol in an oil bath at 110 °C with magnetic stirring for 30 min. The resulting PDES was named according to the molar ratio of the components: HC_1 (CA:HDO=1:2), HC_2 (CA:HDO =1:1), HC_3 (CA:HDO =2:1) or HC_4 (CA:HDO =2:3), and after aggregations were named P_1, P_2, P_3 and P_4. HC_1 and HC_2 were stable homogeneous solutions, whereas HC_3 was not. Each of the three PDES was then poured into a mold and placed in an oven at 110 °C for 20 hours to test the film-forming ability. As a result, only P_2 and P_4 could be polymerized into a film that can be peeled off. However, the mechanical properties of P_4 are very poor.

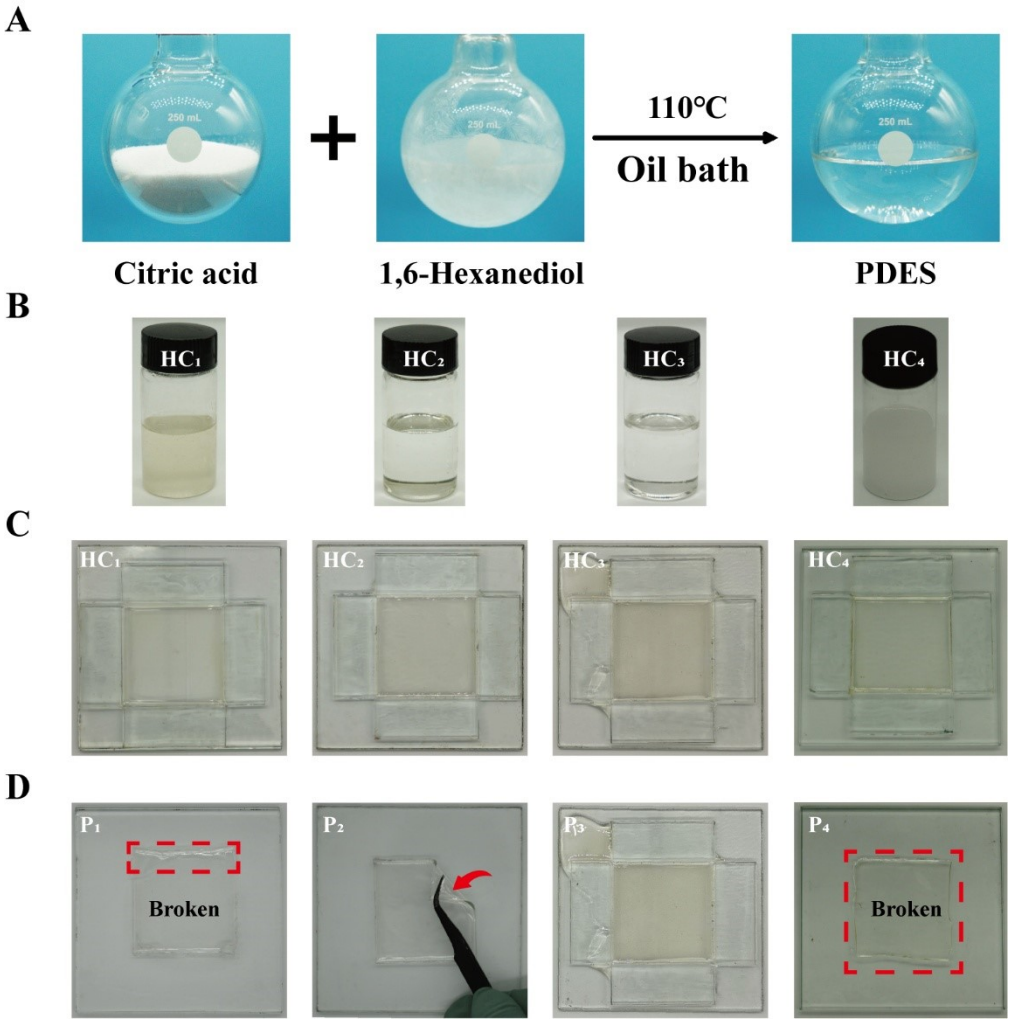

Figure S1. A. Synthesis of PDES. B. PDES synthesized at different molar ratios. C. PDES after polymerization in molds in an oven at 110 °C for 20 hours. D. Comparison of the film-forming ability of polymerized PDES.

From the DSC testing on HC_2 (Figure S2A), it can be observed that the melting point of HC_2 is 33.27°C, which is lower than that of CA (153–159°C) and HDO (43°C). Primary experimental validation confirmed the successful formulation of a homogeneous solution through the combination of CA and HDO.

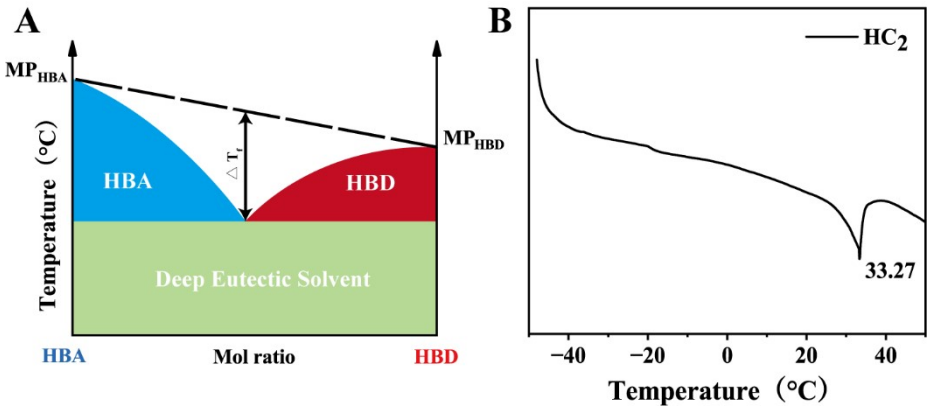

Figure S2. A. Schematic representation of the eutectic point between HBA and HBD.[1] B. DSC testing of HC_2.

We have conducted liquid FTIR tests on the PDES before polymerization to confirm its successful synthesis. As shown in Figure S3, the characteristic peaks of 1,6-hexanediol at 3383 cm^{-1} and 3319 cm^{-1} (corresponding to O-H stretching vibrations) were replaced by a broad peak at 3343 cm^{-1} after the reaction at 110°C for 30 minutes. The observed peak broadening suggests stronger hydrogen bonding within the solvent system. Additionally, the sharp peaks observed in the pure components were no longer present in the HC_2 sample. These findings are highly consistent with previously reported literature[2, 3], suggesting the formation of dense hydrogen-bonding networks, which further confirms the successful synthesis of the DES.

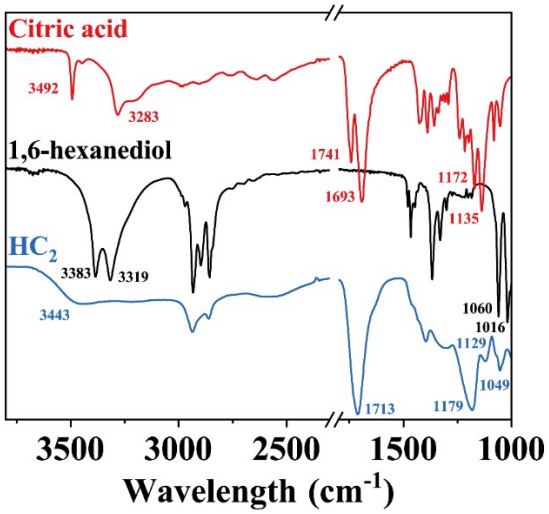

Figure S3. FTIR spectra of citric acid, 1,6-hexanediol, and HC_2

From the figure S4A, it can be observed that new peaks emerge at 1720 cm^{-1} and 1200 cm^{-1} (corresponding to the C=O stretching vibration of ester bonds and the asymmetric C-O-C stretching vibration, respectively). The appearance of these two peaks confirms the successful synthesis of polyester. Subsequently, we amplified the characteristic peak at 1200 cm^{-1} (Figure. S4B), and the results show that the peak intensity of P_4 is weaker than that of P_2. This indicates that adding additional HDO beyond the HC_2(molar ratio CA: HDO = 1:1) ratio does not promote the esterification reaction. The PDES formulation with optimal film-forming properties HC_2 was selected for subsequent experiments and designated as HC.

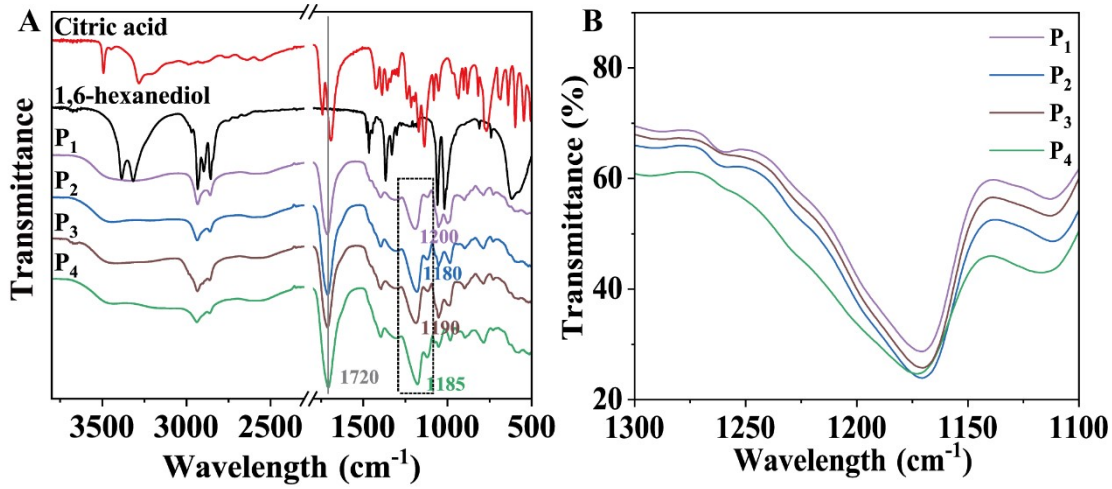

Figure S4 Infrared spectra of P_1, P_2, P_3, P_4, citric acid, and 1,6-hexanediol.

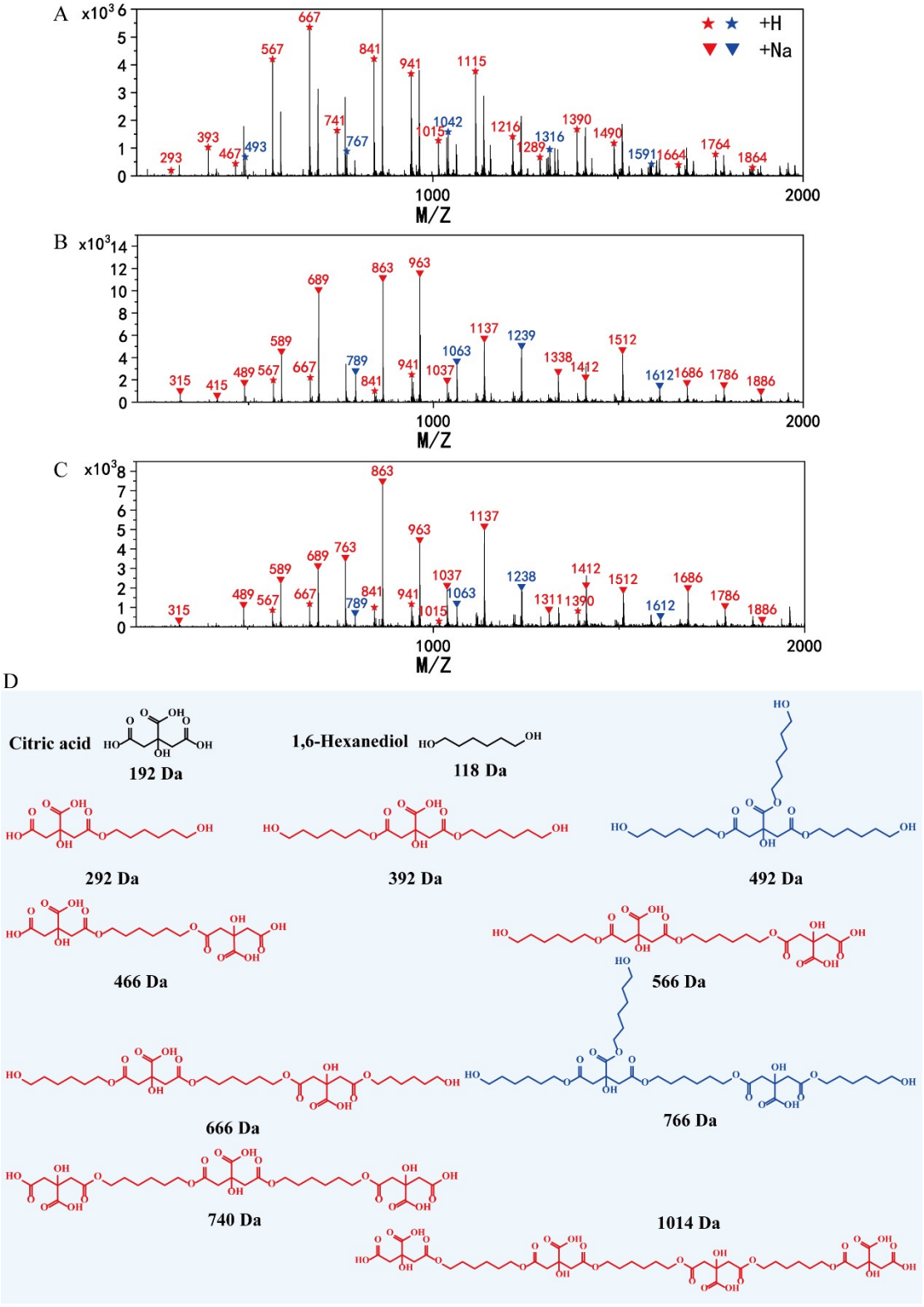

Figure S5. LC-MS spectra of samples obtained after 1 hour (A), 3 hours (B), and 5 hours (C) of esterification of HC_2 at 110 °C. D. Possible structures in the samples. Pentagrams and triangles were used to label the +H and +Na peaks (molecular weight minus 1 or 23 to get the molecular weight of the corresponding structures in the samples). Those in blue represent the doubtless molecular structures in the samples where the carboxyl group of the side chain of citric acid was also esterified, and those

in red represent the possible molecular structures in the samples where the esterification sites of citric acid could not be identified. It was concluded that in the molecular weight range of 0~2000 Da, the samples appeared in ordered chain structures with up to one carboxyl group of the side chain of citric acid esterified in each molecular structure.

The inherent insolubility of the HC in conventional deuterated solvents presents significant analytical challenges. To circumvent this limitation while maintaining structural relevance, we strategically synthesized well-defined HC oligomers through (HC_2) through precise control of reaction parameters (110°C, 1 h and 3 h).

Comprehensive ^{1}H NMR analysis was conducted in deuterated trifluoroacetic acid, the sole solvent system found to adequately dissolve the HC oligomers. The corresponding spectra reveal, presented in Supplementary Materials, reveal three diagnostically significant resonances at 1.72 ppm, 2.01 ppm, and 4.53 ppm (references for NMR assignment). Notably, extending the polymerization duration to 3 h induced a marked intensification of the CH_2 proton signal within ester functionalities. This temporal evolution of spectral features provides direct evidence of progressive polycondensation between citric acid and 1,6-hexanediol, thereby conclusively validating the polyester architecture proposed in our MS-based structural analysis.

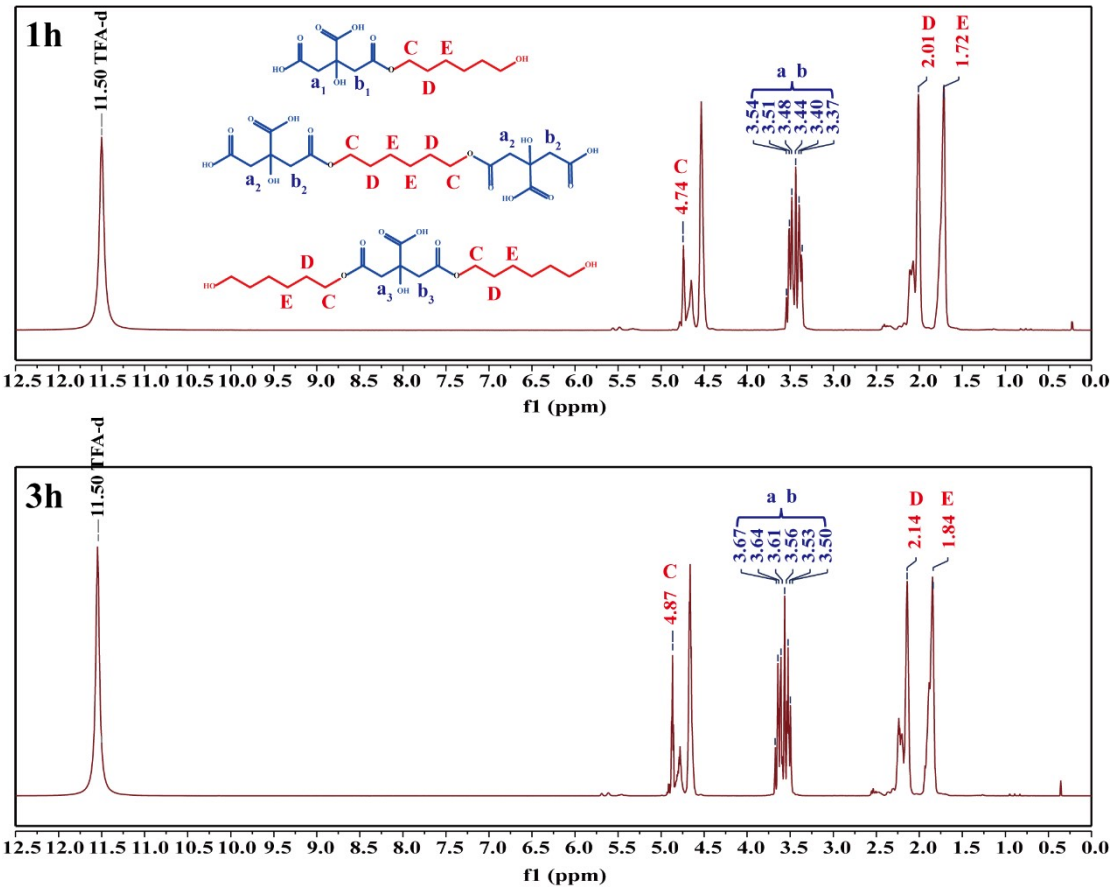

Figure S6. ^{1}H NMR spectra of HC oligomers obtained after 1 hour and 3 hours esterification of HC_2 at 110 °C.

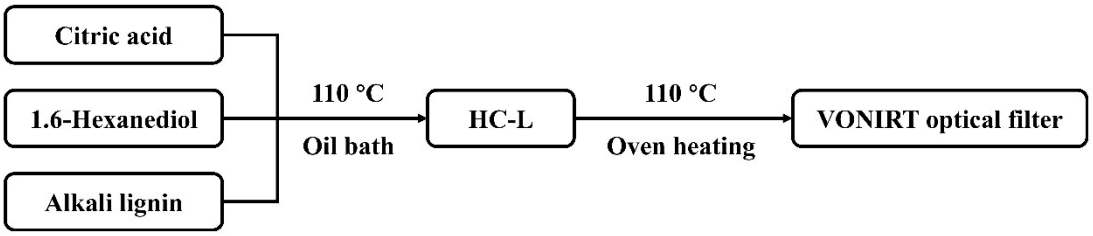

Figure S7. Steps for preparing VONIRT materials. A certain mass fraction (5%, 10%, 15%) of AL was added to a round-bottomed flask containing HC solution, heated in an oil bath at 110 °C, and stirred continuously with a stirring paddle (1000 rpm) for 2 hours until the lignin was dissolved entirely. The dissolved lignin solution was poured into a mold and further reacted at 110 °C to obtain a lignin-based polyester optical filter, noted as 5% L, 10% L, or 15% L, depending on the lignin content. The calculation formula is as follows:

$$Lignin\ content\ (wt\%)\ = \frac{Lignin\ quality}{HC\ quality} * 100\%$$

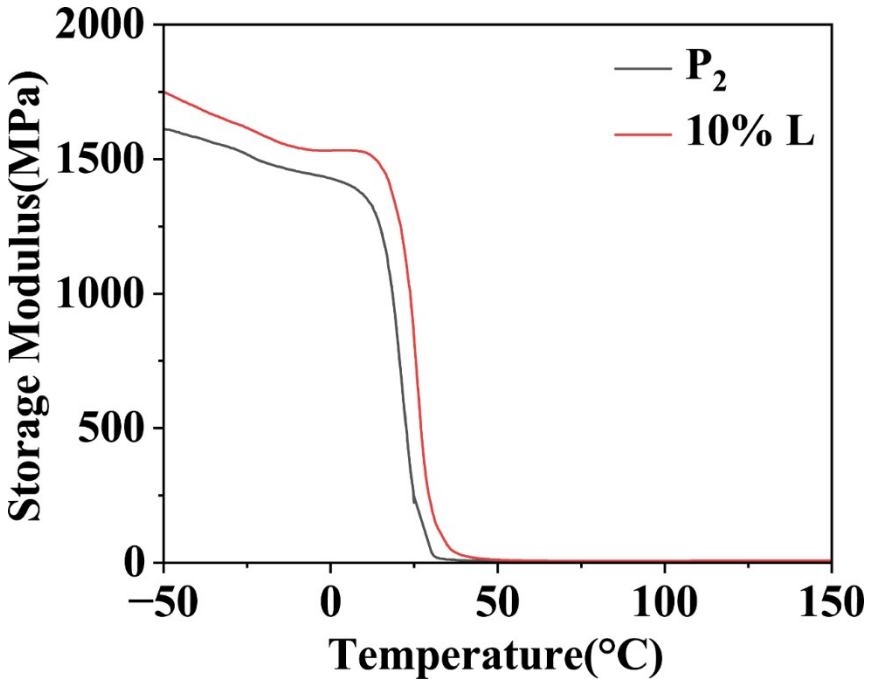

Figure S8. Storage Modulus versus Temperature for P_2 and 10%L

Crosslinking density (ν) is defined as the number of moles of effective crosslinking points per unit volume of the material (unit: mol/m³). According to rubber elasticity theory , in the high elastic state (rubbery state)[4], the relationship between storage modulus (E') and crosslinking density is expressed as:

$$E' = 6\nu RT$$

where R is the universal gas constant (8.314 J/(mol·K)), T denotes the absolute temperature (in Kelvin, K), and ν represents the crosslinking density. Therefore, it can be derived that:

$$\nu = \frac{E'}{6RT}$$

The DMA results reveal that both P_2 and 10% L samples exhibit stabilized storage modulus (E') after 50°C, reaching the rubbery plateau region. Based on this observation, the E' values at 100°C (6.29 MPa for P_2 and 7.19 MPa for 10%L) were selected for crosslinking density calculation. According to the formula, the calculated crosslinking densities are 337.9 mol/m³ for P_2 and 386.3 mol/m³ for 10%L. The increased crosslinking density upon lignin incorporation clearly demonstrates that lignin facilitates the crosslinking reaction.

To verify the impact of lignin dissolution on material properties, we conducted a control experiment where lignin remained undissolved (PDES was pre-reacted at 110°C for 3 hours before adding lignin) and performed SEM testing (Figure S9C). As evident from Figure S9C, the material prepared with undissolved lignin exhibits severe lignin condensation, manifesting as particulate aggregates within the polyester matrix. In contrast, Figure R8B of the 10% L sample demonstrates no detectable lignin agglomerates even at 5000×, 10,000× and 20,000× magnifications, confirming that the lignin remains uniformly dispersed without undergoing re-condensation during the esterification process.

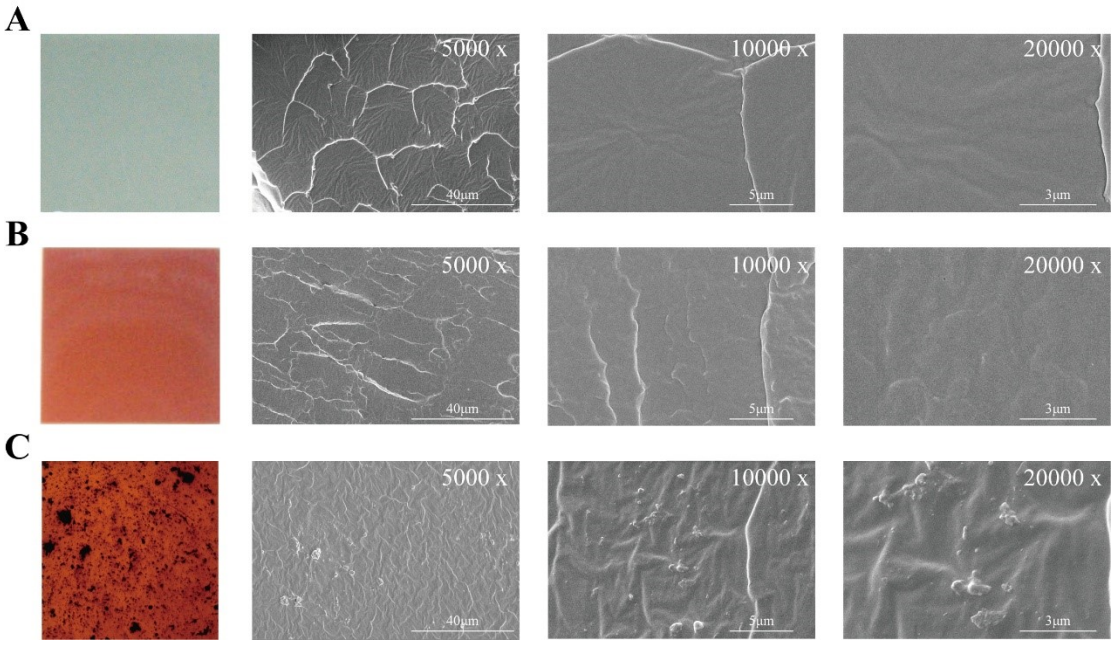

Figure S9. Photographic images and cryo-fractured cross-sectional SEM micrographs of P_2 (A), 10% L (B), and 10% (C) undissolved lignin-containing polyester films.

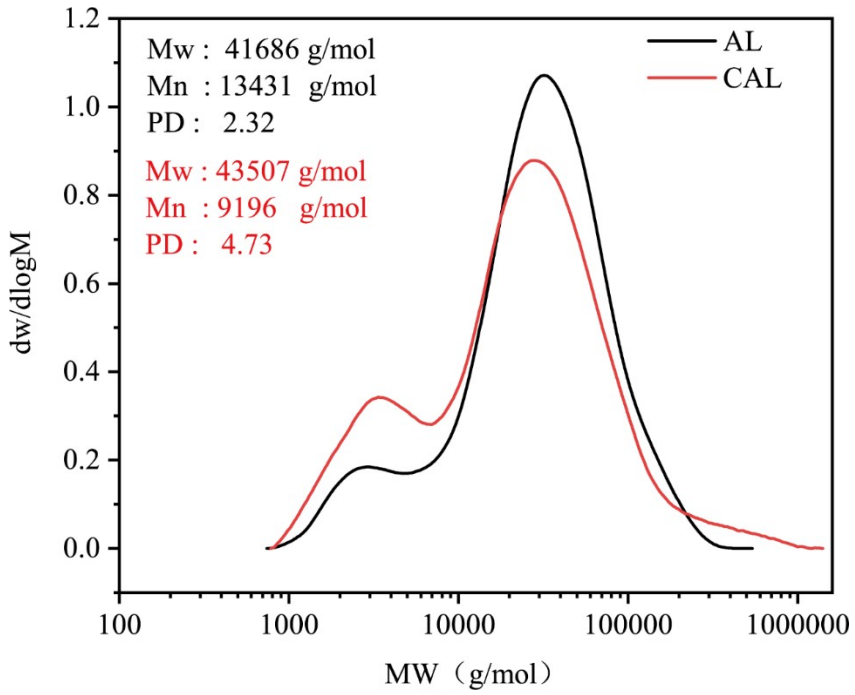

Figure S10. GPC analysis for lignin before and after CA treatment.

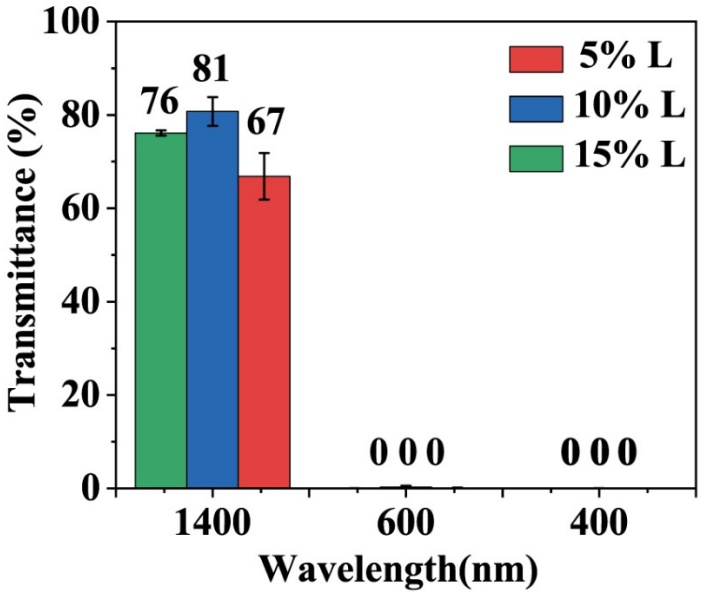

FigureS11. Transmittance of films with different lignin contents at 1400, 600, and 400 nm.

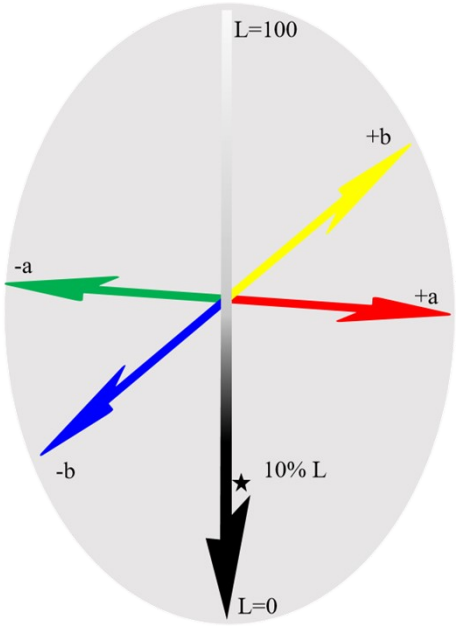

Figure S12. CIE 1976 3D L*a*b* plot of values measured for the color of 10% L optical filter. A color space defined by the International de l'éclairage (CIE) in 1976, where the three measurement parameters represent lightness (0 = black, 100 = white), red-green balance (+a* = red and -a* = green), and yellow-blue balance (+b* = yellow and -b* = blue), respectively.

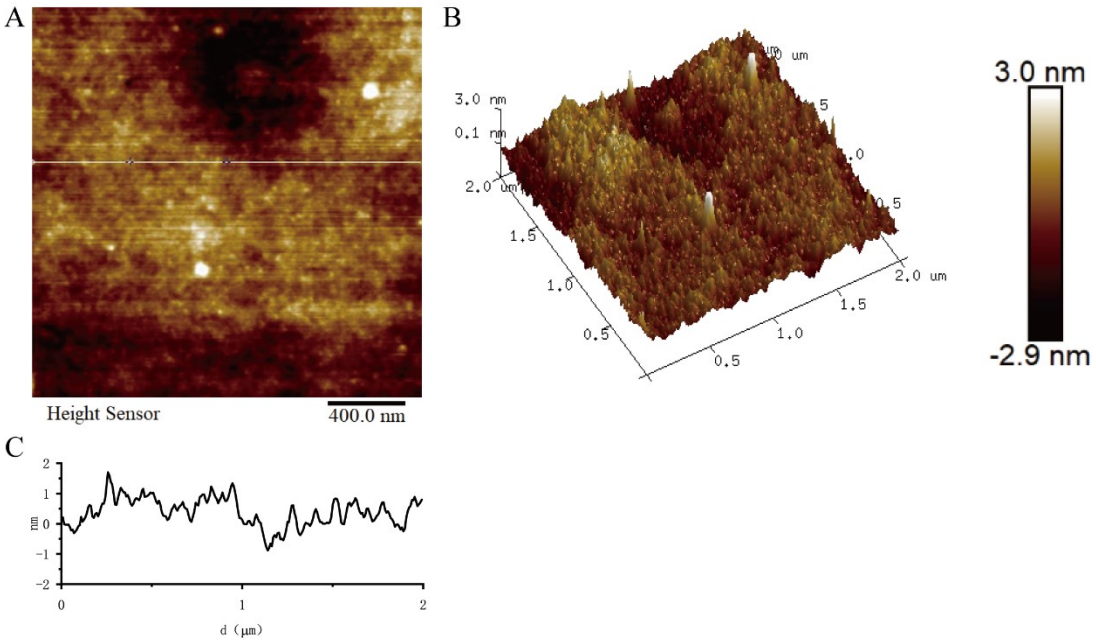

Figure S13. AFM images of 10% L optical filter. The images show that the height difference of the filter surface does not exceed 6 nm, which indicates that the filter surface is flat enough to reduce light scattering in favor of NIR light transmission.

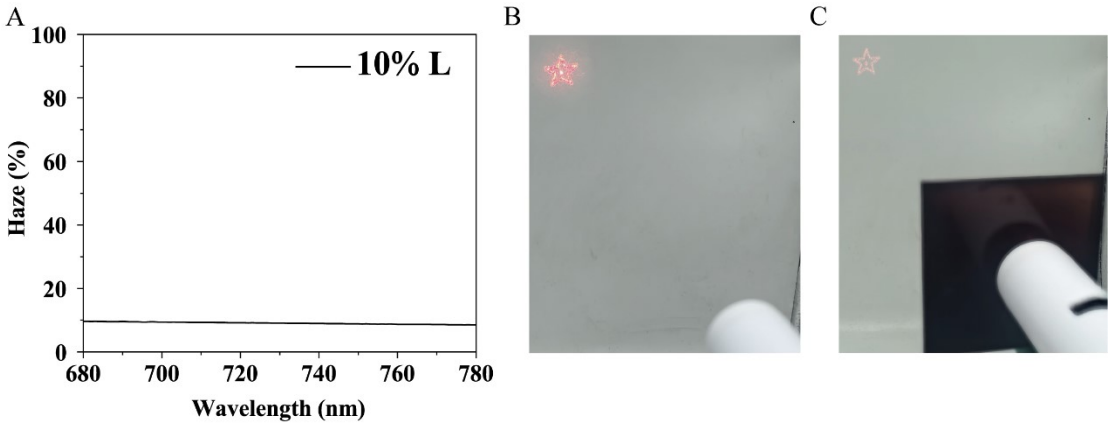

Figure S14. A. Haze of 10% L optical filter in the range of 680~780 nm. B and C. Infrared light test for the haze of 10% L optical filter.

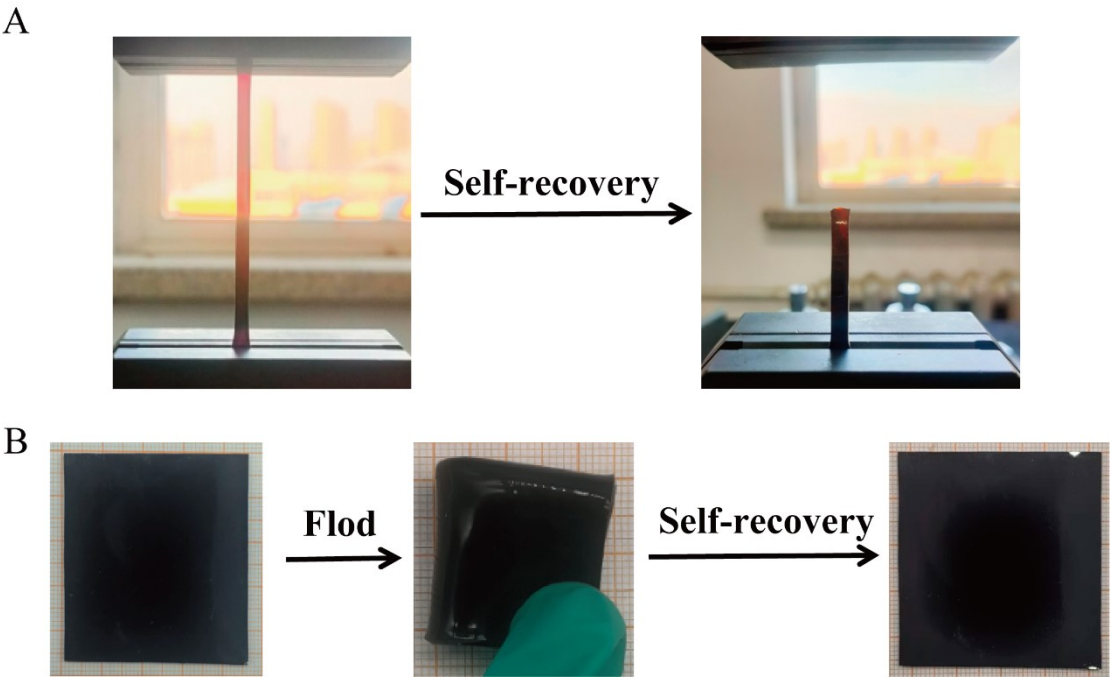

Figure S15. Demonstration of the resilience of 10% L optical filter. 10% L optical filter quickly returned when stretched to break on a universal testing machine or folded in half twice and then released.

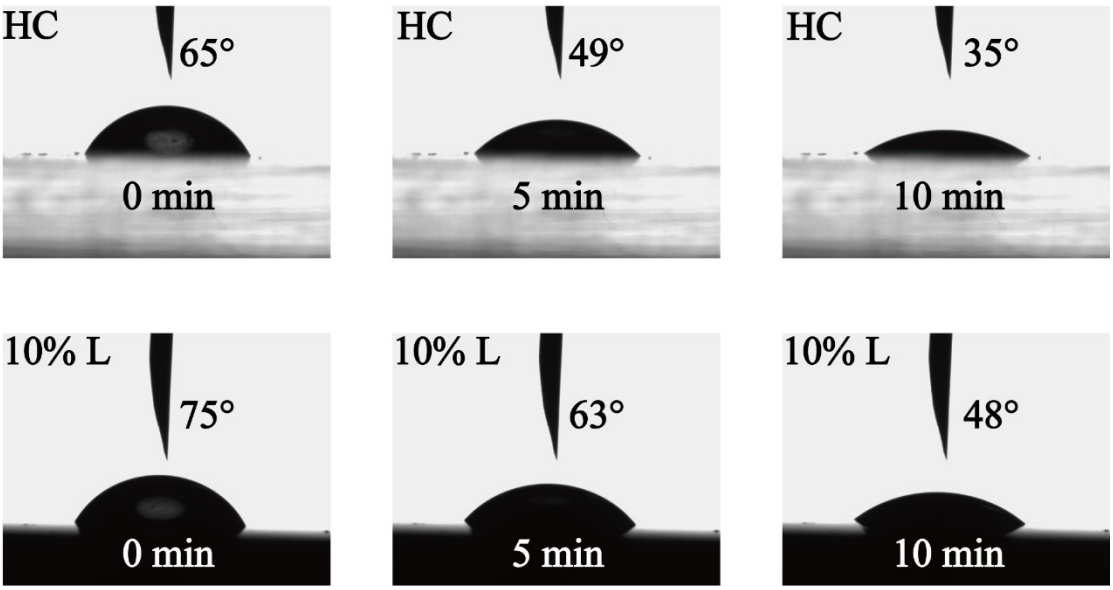

Figure S16. Water contact angle test for HC and 10% L optical filter. The addition of lignin increased the water contact angle of 10% L optical filter, indicating enhanced hydrophobicity.

1. Y. Liu, W. Chen, Q. Xia, B. Guo, Q. Wang, S. Liu, Y. Liu, J. Li and H. Yu, *ChemSusChem*, 2017, **10**, 1692-1700.
2. H. V. D. Nguyen, R. De Vries and S. D. Stoyanov, *ACS Sustainable Chemistry & Engineering*, 2020, **8**, 14166-14178.
3. S. L. Perkins, P. Painter and C. M. Colina, *Journal of Chemical & Engineering Data*, 2014, **59**, 3652-3662.
4. C. T. Hiranobe, G. D. Ribeiro, G. B. Torres, E. A. P. d. Reis, F. C. Cabrera, A. E. Job, L. L. Paim and R. J. d. Santos, *Materials Research*, 2021, **24**.